LETTER TO THE EDITOR

Order from disorder in the double-exchange model

Nic Shannon[1] **and Andrey V Chubukov**[2]

[1] Max-Planck-Institut für Physik komplexer Systeme, Nöthnitzer Str. 38, 01187 Dresden, Germany
[2] Department of Physics, University of Wisconsin, Madison, 1150 Univ. Av., Madison, WI 53706, USA

Abstract
The magnetic excitations of the double-exchange (DE) model are usually discussed in terms of an equivalent ferromagnetic Heisenberg model. However this equivalence is valid *only* at a quasi-classical level—we show that both quantum and thermal corrections to the magnetic properties of the DE model differ from *any* effective Heisenberg model because its spin excitations interact only indirectly, through the exchange of charge fluctuations. We also find that the competition between ferromagnetic DE and an antiferromagnetic superexchange provides a new example of an 'order from disorder' phenomenon—an intermediate spin configuration (either a canted or a spiral state) is selected by quantum and/or thermal fluctuations.

(Some figures in this article are in colour only in the electronic version)

1. Introduction

Many magnetic systems of current experimental interest, for example the colossal magnetoresistance (CMR) manganites [1, 2] and pyrochlores [3], consist of itinerant electrons interacting with an array of localized magnetic moments with spin S. The simplest models of these systems comprise a single tight-binding band of electrons interacting with localized core spins by a Hund's rule exchange interaction $J_H \gg t$

$$\mathcal{H}_\infty = -t \sum_{\langle ij \rangle \alpha} c^\dagger_{i\alpha} c_{j\alpha} - J_H \sum_{i\alpha\beta} \vec{S}_i \cdot c^\dagger_{i\alpha} \vec{\sigma}_{\alpha\beta} c_{i\beta} \tag{1}$$

where the sum $\langle ij \rangle$ is restricted to neighbouring sites. The ground state of this model must generally be ferromagnetic (FM), since Hund's rule requires the spin of itinerant electrons to be locally aligned with the core spins, and the kinetic energy of electrons is in turn minimized by making all the electron spins parallel. This effect is usually called 'double exchange' (DE), and the model of equation (1) is referred to as the double-exchange ferromagnet (DEFM).

In addition to DE interaction, core spins may also interact via a direct superexchange

$$\mathcal{H}_2 = J_2 \sum_{\langle ij \rangle} \vec{S}_i \cdot \vec{S}_j. \tag{2}$$

In CMR materials, J_2 is sometimes positive (antiferromagnetic (AF)), in which case superexchange competes directly with the DE mechanism.

In the classical limit $S \to \infty$, the FM ground state favoured by $\mathcal{H}_1$ is stable for all $J_2 < J_1$ where $J_1 = \bar{t}/4S^2$, and $\bar{t}$ is the average kinetic energy per bond in the lattice (see e.g. [4–8]). For larger values of J_2, the competition between AF exchange and the kinetic energy of electrons gives rise to a uniform phase where neighbouring spins are misaligned by an angle θ, with $\cos\theta/2 = J_1/J_2$ [4]. However, θ alone does not specify a particular intermediate configuration—there exist an infinite set of classically degenerate states with the same θ. The two ends of this set are a two-sublattice canted phase and a spiral phase [4]. This degeneracy reflects the local classical symmetry—we can take any spin on the A sublattice of the canted phase and rotate it about the direction of magnetization of the B sublattice without changing θ. Since it costs no energy to make such an excitation, the system cannot distinguish between different states, and should be magnetically disordered even at[3] $T = 0$.

The argument about degeneracy, however, does not hold at finite S, and we anticipate that quantum and/or thermal fluctuations will remove the degeneracy and enable the system to choose its true ground state. Such 'order from disorder' effects have been widely discussed in the context of magnetic insulators, e.g. for Kagomé antiferromagnets [9]—but not in the context of interacting electron systems.

The analysis of 'order from disorder' effects in systems with *local* classical symmetry is generally rather involved as one has to expand around infinitely degenerate state [9]. For DE systems, one, however, can determine which of the classically degenerate states is selected by fluctuations by looking for the wavevector Q^* at which the spin-wave excitation about the FM state first becomes negative (provided that the system does not undergo a first-order transition into an inhomogeneous state). The softening at $Q^* = 0$ implies the instability towards a spiral phase, while the softening at $Q^* = (\pi, \pi, \pi)$ implies the instability towards a canted phase. This question *cannot* be answered at a semi-classical level, since to $\mathcal{O}(\infty/S)$ the Hamiltonian of equation (1) and (2) can be mapped onto an effective nearest-neighbour Heisenberg model: $(J_1 - J_2) \sum_{\langle ij \rangle} \vec{S}_i \cdot \vec{S}_j$ (see e.g. [4–8]), and the spin-wave spectrum vanishes identically for $J_1 = J_2$. Once quantum effects are restored, however, fluctuations generate a long-range interaction between spins which breaks the local classical symmetry. As a result the mapping onto a nearest-neighbour Heisenberg model breaks down. The issue then reduces to how quantum and thermal corrections to the spin-wave spectrum of equation (1) distinguish between the DEFM and nearest-neighbour Heisenberg ferromagnet (HFM). It is this question that we address.

The analysis in the FM state is easier to perform than an 'order from disorder' study in either canted or spiral states as the FM state is not degenerate and the expansion around it should be free from singularities (in practice, this implies that corrections to classical dispersions form regular series in $1/S$). On the other hand, 'order from disorder' effects for classically degenerate states are generally stronger because of singularities (for Kagomé antiferromagnets, the expansion parameter is $1/S^{2/3}$ rather than $1/S$ [9]). From this perspective, our analysis will only indicate which state is selected near a FM boundary. However, by continuity, we anticipate that the same state will be selected for all J_1/J_2.

---

[3] We have performed a classical spin-wave analysis for the canted phase of the DEFM and indeed found that $\omega_{sw}(q) \equiv 0$ for all q as it should be for a locally degenerate ground state.

In order to perform calculations beyond the quasi-classical limit, we introduce a new spin-wave expansion which takes correct account of the dual itinerant/localized nature of electrons in the DEFM. Using this expansion we evaluate the spin-wave spectrum of the DEFM at $T = 0$ and a finite temperature and show that it differs from that in an HFM. Our $T = 0$ results agree with earlier numerical [10–12] and analytical studies [13–15], but we shall explain from a physical point of view why the DEFM differs from the HFM. Our results at finite T are entirely new.

2. Transformation of Hamiltonian

Given that the Hund's rule coupling J_H is the largest energy scale in the problem it is desirable to diagonalize this term first and project out all electrons not locally aligned with the core spins. We should also define spin-wave excitations such that they are the true Goldstone modes of the order parameter, i.e. transverse fluctuations of the composite spin $\vec{\mathcal{S}}_i = \vec{S}_i + \frac{1}{2} \sum_{\alpha\beta} c^\dagger_{i\alpha} \vec{\sigma}_{\alpha\beta} c_{i\beta}$. We accomplish both of these goals by the following procedure: (i) introducing new Fermi operators f_i and p_i which create electronic 'up' and 'down' states aligned with the quantization axis of the composite spin and (ii) generalizing the Holstein–Primakoff transformation to the case where the length of the spin is itself an operator, introducing a corresponding bosonic operator $\tilde{a}_i$. To capture the essential physics of the DEFM it is sufficient to know the inverse transformation to $\mathcal{O}(1/S)$:

$$a = \tilde{a}\left(1 + \frac{p^\dagger p - f^\dagger f}{4S}\right) - \frac{f^\dagger p}{\sqrt{2S}} + \mathcal{O}(1/S^{3/2})$$

$$c_\uparrow = f\left(1 - \frac{\tilde{a}^\dagger \tilde{a} + p^\dagger p}{4S}\right) - \frac{p\tilde{a}^\dagger}{\sqrt{2S}} + \mathcal{O}(1/S^{3/2}) \tag{3}$$

$$c_\downarrow = p\left(1 - \frac{\tilde{a}^\dagger \tilde{a} + ff^\dagger}{4S}\right) + \frac{f\tilde{a}}{\sqrt{2S}} + \mathcal{O}(1/S^{3/2})$$

where a is the Holstein–Primakoff boson associated with the core spin. A more complete discussion of the transformation will be given elsewhere [16]; here we simply state that the transformation and its inverse are unitary, and satisfy all required (anti-) commutation relations, for example $\{f, f^\dagger\} = \{p, p^\dagger\} = [\tilde{a}, \tilde{a}^\dagger] = 1$, $[f, \tilde{a}] = \{f, p\} = 0$ etc, and that our expansion procedure reproduces all features of an exact solution of the DE model on two sites [17]. Substituting this transformation into equation (1), we find that the Hund's rule term reduces to

$$\mathcal{H}_1 = -\frac{J_H S}{2}\left[f^\dagger f - p^\dagger p\left(1 + \frac{1}{S}\right) + \frac{f^\dagger f p^\dagger p}{S}\right] \tag{4}$$

where the sum over lattice sites has been suppressed. Clearly p operators describe low-spin, high-energy excitations and can safely be dropped. Simultaneously, the hopping term in equation (1) transforms into the Hamiltionian which describes a single band of spinless fermions interacting with (initially dispersionless) Holstein–Primakoff bosons. On Fourier transform we obtain

$$\mathcal{H}_t = \sum_{k_1}(\epsilon_1 - \mu)f^\dagger_1 f_1 + \frac{1}{N}\sum_{k_1 \ldots k_4} V^{13}_{24} f^\dagger_1 f_2 \tilde{a}^\dagger_3 \tilde{a}_4 \delta_{1+3-2-4} + \cdots \tag{5}$$

$$V^{13}_{24} = \frac{1}{4(S+\frac{1}{2})}\left[\left(1 + \frac{1}{8S}\right)(\epsilon_{1+3} + \epsilon_{2+4}) - (\epsilon_1 + \epsilon_2)\right] \tag{6}$$

where all energy scales are set by the electron dispersion $\epsilon_k = -zt\gamma_k$.
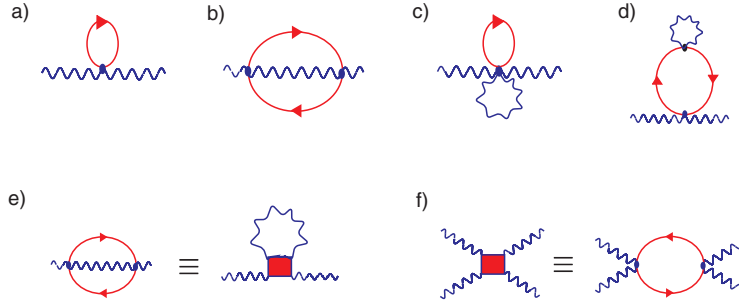
Figure 1. (*a*)–(*d*) Diagrams contributing to spin-wave self-energy in a ferromagnet to order $\mathcal{O}(1/S^2)$. Only diagrams (*a*) and (*b*) are physically relevant. (*e*), (*f*) The representation of diagram (*b*) via an effective four-boson interaction mediated by the charge susceptibility (a particle–hole polarization bubble).
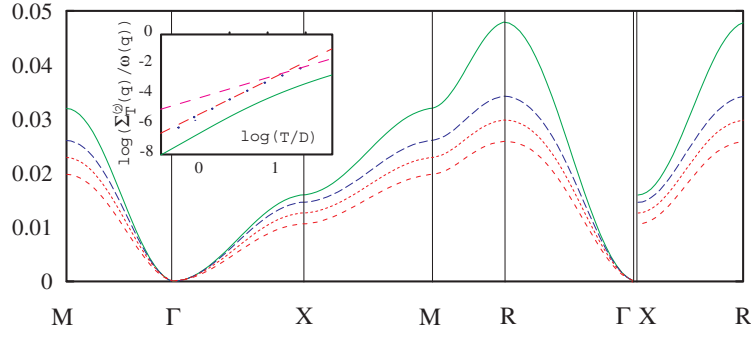
3. Spin-wave dispersion

The Hamiltonian of equation (5) does not contain a bare spin-wave dispersion—it emerges only through interaction with electrons. Accordingly, the spin-wave propagator $D(q, \Omega) = [\Omega - \Sigma(q, \Omega)]^{-1}$ where $\Sigma(q, \Omega)$ is the bosonic self-energy. The leading 'semi-classical' spin-wave dispersion originates from the fact that the oscillations of the core spins destroy perfect alignment of the spins of the itinerant electrons, which increases their kinetic energy. Diagrammatically this corresponds to the process in figure 1(*a*), which gives

$$\Sigma^{(1a)}(q) = zJ_1 S[1 - \gamma_q] \qquad J_1 = \frac{t}{4S^2} \frac{1}{N} \sum_{\vec{k}} n_k \gamma_k. \tag{7}$$

At this level we indeed reproduce the spin-wave spectrum of a nearest-neighbour HFM.

The equivalence between DEFM and HFM is, however, lost beyond the semi-classical approximation. There are four self-energy contributions at $\mathcal{O}(1/S^2)$, one from each of the diagrams in figures 1(*a*)–(*d*). At finite temperature these also include a contribution from a sixfold term in $\mathcal{H}_t$, omitted from equation (5). However we verified that there is considerable cancellation between terms, and all new physical effects originate from the diagram in figure 1(*b*). This diagram can be thought of as a first-order bosonic self-energy due to effective four-boson interaction mediated by fermions (see figures 1(*e*) and (*f*)). The difference between DEFM and the Heisenberg model then can be readily understood on general grounds. Indeed, in an HFM, the four-boson vertex does not depend on frequency and scales as q^2l^2 [18], where $q, l \ll 1$ are the bosonic momenta. In the DEFM, the interaction is mediated by the dynamical charge susceptibility of the Fermi gas, $\Pi(q - l, \omega_p - \omega_l)$ (see figure 1(*e*)), which is generally a complex function of momentum and frequency. This gives rise to two effects which both are relevant to our analysis. (i) $\Pi(q - l, \omega_p - \omega_l)$ has a branch cut, which gives rise to a nonzero renormalization of the spin-wave dispersion at $T = 0$. (ii) The static $\Pi(q - l, 0)$, relevant to thermal corrections to the dispersion at $T < J_1 S$, scales differently from J_1: at small p_F, $J_1 \propto p_F^3$, while $\Pi(q - l) \propto p_F$ at $q, l_{typ} \ll p_F$ and $\Pi(q - l) \propto p_F^3/|q - l|^2$ for $|q - l| \gg p_F$. Accordingly, at small doping x, when typical q and l exceed p_F, the momentum dependence of $\Pi(q - l)$ causes thermal self-energy corrections in the DEFM to have a different functional form from those in the HFM.

Figure 2. Dispersion of spin waves in a cubic DEFM with electron doping $x = 0.7$ and spin $S = 3/2$, in units of the electron bandwidth $2zt = 1.0$. Solid curve—dispersion of classically equivalent Heisenberg model. Dashed curves—dispersion of DEFM including leading quantum and thermal corrections for (top to bottom) $T = 0$, $T = 2D/3$ and $T = D$, where $D = 12J_1S$ is the bandwidth of spin-wave excitations. Inset—thermal corrections to spin-wave dispersion in a DEFM for $q = (\pi/2, \pi/2, \pi/2)$ (points) compared with those for an equivalent HFM (solid curve). Dashed curves represent $T^{5/2}$ and $T^{3/2}$ power laws as a guide to the eye.

4. Quantum corrections at $T = 0$

The leading correction to equation (7) at $T = 0$ is

$$\Sigma^{(2)}_{T=0}(q) = -\frac{zt}{4S^2}\frac{1}{N^2}\sum_{p,l} n_F(p)(1 - n_F(l))\left[(1 - \gamma_q)\gamma_p\frac{\gamma_p + \gamma_l}{\gamma_p - \gamma_l} - \frac{\gamma_p^2 - \gamma_{q+p}^2}{\gamma_p - \gamma_l}\right] \tag{8}$$

where $n_F(l) = n_F(\epsilon_l)$ is a Fermi function which, for $T = 0$, reduces to a step function. The first term in equation (8) simply renormalizes the classical Heisenberg-like spin-wave dispersion, while the second has a dependence on q which is quite different from that in the nearest-neighbour Heisenberg model. This term is either positive or negative throughout the Brillouin zone (BZ), depending on the electronic density, and is symmetric under $\vec{q} \to \vec{\pi} - \vec{q}$, where $\vec{\pi} = (\pi, \pi, \pi)$. Along the zone diagonal, it reduces to $(zt/4S^2)I(x)[1 - \cos(2q)]$, where $I(x) = (1/N^2)\sum_{pl} n_F(p)(1 - n_F(l))(\gamma_p^2 - \gamma_{p+\pi/2}^2)/(\gamma_p - \gamma_l)$ changes sign twice as a function of x. This form of the correction to Heisenberg dispersion is comparable to that found in numerical studies of the DE model on a ring [10] and with equivalent analytical results [15]. The renormalized spin-wave dispersion of the DEFM at $T = 0$ is shown in figure 2. A notable feature is the marked suppression of spin-wave dispersion for all symmetry directions lying on the boundary of the BZ.

We are now in a position to answer the question posed above about order from disorder effects. We find that for intermediate densities $0.31(7) < x < 0.92(7)$ in two dimensions and $0.31(7) < x < 0.94(2)$ in three dimensions, $I(x) < 0$ and quantum effects cause a relative softening of spin-wave modes near the zone centre. This means that the first instability of the DEFM with competing AF exchange interactions is against a spiral phase with $Q^* \approx (0, 0, 0)$. On the other hand, for a small density of electrons (or holes), $I(x) > 0$, and quantum effects instead lead to a relative softening of modes near the zone boundary. In this case the spin-wave spectrum first becomes unstable against a canted spin configuration with $Q^* = (\pi, \pi, \pi)$. These results are in almost perfect agreement with numerical studies [12].

5. Corrections to the dispersion at finite T

In a Heisenberg model, the thermal self-energy has the form $\Sigma_T^{HFM}(q) = -2zJ_1S(1-\gamma_q)$ $\beta(T)/4S^2$ where $\beta(T) = 1/N \sum_l n_B(l)(1-\gamma_l)$ [18], where $n_B(l) = n_B(\epsilon_l)$ is a Bose function. At $T \ll J_1S$, typical l are small, and $\beta(T) \approx (\zeta(5/2)/32\pi^{3/2})\,(T/J_1S)^{5/2}$. Most importantly, the temperature effects do not change the form of spin-wave dispersion, which still remains proportional to $1 - \gamma_q$. In the case of the DEFM we obtain

$$\Sigma_T^{(2)}(q) = -\frac{zt}{4S^2}\frac{1}{N^2}\sum_{p,l} n_B(l)\frac{n_F(p+m/2) - n_F(p-m/2)}{\gamma_{p+m/2} - \gamma_{p-m/2}}$$

$$\times (\gamma_{p-m/2} - \gamma_{p+q-m/2})(\gamma_{p+m/2} - \gamma_{p+q-m/2}). \tag{9}$$

Here $\vec{m} = \vec{q} - \vec{l}$, and $n_B(l) = n_B(\Omega(l))$ and $n_F(k) = n_F(\epsilon_k)$. The behaviour of $\Sigma_T^{(2)}(q)$ depends on doping, and is quite different in the limits of small and large doping. We analysed equation (9) in detail analytically for $T \ll J_1S$ and $x \ll 1$ and found that $\Sigma_T^{(2)}(q) \propto q^2 T^{5/2}$ (as in HAF) only at very small $q \ll p_F$. Even in this limit, the overall factor is larger than in HFM by a factor $\propto 1/p_F^2$ (recall that $J_1 \propto p_F^3$). At arbitrary q, the self-energy deviates down from $(1 - \gamma_q)T^{5/2}$ form due to the reduction of the charge susceptibility. For $q \gg p_F$ we obtained

$$\Sigma_T^{(2)}(q) = \frac{t\,p_F^3}{24\pi^2 S^2 N}\sum_l n_B(l)l^2\left[1 + \gamma_q - \frac{1}{3}\frac{1-\gamma_{2q}}{1-\gamma_q}\right]. \tag{10}$$

We see that $\Sigma_T^{(2)}(q) \propto p_F^3 T^{5/2}$ loses q^2 dependence. Comparing this result with that at $q < p_F$, we see that $\Sigma_T^{(2)}(q)$ is *reduced* by p_F^2/q^2, precisely as anticipated on general grounds.

At larger x, we found numerically that the thermal corrections to spin-wave dispersion in the DEFM have a similar temperature dependence to those in the HFM, but are substantially larger, and are not proportional to $1 - \gamma_q$ for large q. For $0.25 < x < 0.75$ (dopings relevant for comparison with the manganites), we find that the thermal self-energy can be approximated by $\Sigma_T^{(2)}(q) \approx \alpha(q, T)\Sigma_T^{HFM}(q)$, where $\alpha(q, T) \approx 5$ is a dimensionless function. Corrections are illustrated in figure 2. In order to more clearly illustrate the trends we consider in this figure temperatures up to $T \sim D = 2zJ_1S$, where D is the bandwidth of the spin-wave excitations. Note, however, that the spin-wave expansion breaks down for $T \gtrsim D$ even if $D < T_c$ [23].

Returning to the issue of order from disorder, we see that for realistic x classical fluctuations primarily soften the dispersion near $q = 0$ and hence favour the spiral state. This implies that the range of dopings where this phase is selected increases with T, at least for $T < J_1S$.

6. Conclusions

In this letter we have used a new spin-wave expansion to explore the extent to which the spin dynamics in a DEFM are the same as in those in an HFM. We found that the two models are equivalent at the classical level ($S \to \infty$), but that both quantum and thermal corrections in the DEFM are different because the interaction between spin waves is mediated by fermions and is qualitatively different from that in an HFM. We studied in the detail the form of quantum and thermal corrections to the spin-wave dispersion in DEFM.

We applied the results to address the issue of which state is selected near the FM instability in the case of competition between ferromagnetic DE and a direct antiferromagnetic superexchange. We found that fluctuations select either a canted state or a spiral state, depending on the electron density.

The softening of zone boundary spin waves has been observed in neutron scattering experiments on the CMR manganites [19] at a *hole* doping $\tilde{x} = 1 - x \sim 0.3$. It has

been suggested that this softening may be due to deviations from Heisenberg behaviour in the DEFM [10, 15, 19], or to another mechanism (e.g. a coupling to phonons [14, 20]). Our analysis essentially eliminates the first possibility as for $x \sim 0.7$ our zero-temperature theory predicts a relative hardening rather than softening of the dispersion at (π, π, π).

The issue left for further studies is a possible phase separation in the non-ferromagnetic regime [21]. To study this possibility in our approach, one has to analyse the sign of the longitudinal susceptibility in, e.g., the canted phase. If it is negative, then the system is unstable towards phase separation [22]. There calculations are clearly called for.

References

[1] Zener C 1951 *Phys. Rev.* **82** 403
[2] Anderson P W and Hasegawa H 1955 *Phys. Rev.* **100** 675
[3] Majumdar P and Littlewood P 1998 *Phys. Rev. Lett.* **81** 1314
[4] de Gennes P-G 1960 *Phys. Rev.* **118** 141
[5] Kubo K and Ohata N 1972 *J. Phys. Soc. Japan* **33** 21
[6] Furukawa N 1994 *J. Phys. Soc. Japan* **63** 3214
[7] Perkins N B and Plakida N M 1999 *Theor. Math. Phys.* **120** 1182
[8] Millis A J, Littlewood P B and Schraimann B I 1995 *Phys. Rev. Lett.* **74** 5144
[9] Harris A B, Kallin C and Berlinsky A J 1992 *Phys. Rev.* B **45** 2899
      Sachdev S 1992 *Phys. Rev.* B **45** 12 377
      Chubukov A V 1992 *Phys. Rev. Lett.* **69** 832
[10] Kaplan T A and Mahanti S D 1999 *Physics of Manganites* ed T A Kaplan and S D Mahanti (New York: Kluwer)
[11] Zang J *et al* 1997 *J. Phys.: Condens. Matter* **9** L157 and references therein
[12] Wurth P and Muller-Hartmann E 1998 *Europhys. J.* B **5** 403
[13] Irkhin V Yu and Katsel'son M I 1985 *JETP* **61** 306
[14] Khaliullin G and Kilian R 2000 *Phys. Rev.* B **61** 3494
[15] Golosov D 2000 *Phys. Rev. Lett.* **84** 3974
      Golosov D 2000 *J. Appl. Phys.* **87** 5804
[16] Shannon N and Chubukov A V, in preparation
[17] Shannon N 2001 *J. Phys.: Condens. Matter* **13** 6371
[18] see e.g., Akhiezer A I *et al* 1968 *Spin Waves* (New York: Wiley)
[19] Hwang H Y *et al* 1998 *Phys. Rev. Lett.* **80** 1316
[20] Furukawa N 1999 *Preprint* cond-mat/9905123
[21] Moreo A, Yunoki S and Dagotto E 1999 *Science* **283** 2034
[22] Shraiman B I and Siggia E 1992 *Phys. Rev.* B **46** 8305
      Chubukov A and Musaelian K 1995 *Phys. Rev.* B **51** 12 605
[23] Vaks V G, Larkin A I and Pikin S A 1968 *Sov. Phys.–JETP* **26** 647